

The development of leukocyte counter using fluorescence imaging analysis

TAISUKE HIRONO^{1,3,*}, KATSUMI YABUSAKI²
AND YUKIO YAMADA³

¹*Electronics and Optics Res. Labs., Kowa Company, Ltd., Research Laboratories, 3-3-1, Chofugaoka, Chofu, Tokyo, 182-0021, Japan*

²*Kowa Research Institute, Kowa Company, Ltd., Japan*

³*Dept. of Mech. Eng. and Intel. Sys., University of Electro-Communications, Japan*

(*author for correspondence: E-mail: t-hirono@kowa.co.jp)

Received 28 January 2005; accepted 2 June 2005

Abstract. Image cytometry centrifugation (ICC) method has been developed and applied to count residual leukocytes in transfusion blood products for quality assurance testing. The standard leukocyte fluorescence image profile was established by averaging the actual fluorescence images of leukocytes. It was used for development of an optimum image analysis algorithm to avoid misinterpretation of the dust contaminated from the environment. The centrifugal concentration process of the ICC method was investigated by a computer simulation, and it was found that it caused leukocyte overlapping and limited the enumeration range. By introducing a double thresholding algorithm to the fluorescence images analysis and correcting the number of the overlapped leukocytes, we succeeded in improving the accuracy and the measurement range up to 25 [WBC/ μ] of the ICC method.

Key words: computer simulation, cytometry, fluorescence image, image analysis, leukocyte counter, transfusion blood product

1. Introduction

Leukocytes contamination during blood transfusion can cause many serious side effects, such as febrile non-haemolytic reactions, graft-versus-host disease, and immunosuppression (Sirchia *et al.* 1987; Handa *et al.* 1992). Blood products providers are recommended to reduce residual leukocytes in transfusion blood products such as platelet concentrates (PC) or red cells (RC) products etc., and seeking useful instruments to count these leukocytes (Adams *et al.* 1997; Dizik 1997; Neumuller *et al.* 1997).

Nageotte hemocytometry is known as a conventional method for counting residual leukocytes in the blood products (AABB Technical Manual 1996). In this method, a dye solution, e.g. Türk solution or Leukoplate etc., is added to the blood sample to stain the leukocytes, and it is injected into the Nageotte chamber. Then, the chamber has to be placed in a humid environment until the whole leukocytes would completely fall onto the bottom of the chamber. Subsequently, it is counted under a microscope

manually. This time-consuming method requires the expertise of trained and experienced examiner for leukocyte recognition.

In 2000, we developed a new method named the image cytometry centrifugation (ICC) method and the instrument to count leukocytes in the blood products (Yabusaki *et al.* 1999, 2000; Nagahashi *et al.* 2000). It is a comparatively quick, easy, and cost-effective procedure. In brief, the ICC method consists of fluorescent staining and centrifugation of blood cells, and computer-aided imaging analysis to identify and count leukocytes.

However, it was found that the ICC method had two problems in practical use. First, dust was found in the blood samples to emit fluorescence from the dye adsorbed on their surfaces. It appears that they were residual cell components other than leukocytes or came from the environment. Unfortunately, they were counted as leukocytes in error by the previous ICC method, so that it had to be improved so as to count correct number of leukocytes. Second, the acceptable level of residual leukocytes was determined to 1×10^6 [WBC/bag] in Japan, while it is up to 5×10^6 [WBC/bag] by the FDA's recommendation in US (Blood Products Advisory Committee 2001). Since the volume of a transfusion bag is 200–400 ml, it corresponds 25 [WBC/ μ l]. Measurement linearity of the ICC method was reported to 100 [WBC/sample volume] in our previous papers. It corresponds 5 [WBC/ μ l] because the required volume of sample is 20 μ l at least, which is insufficient. The linearity should be required up to 25 [WBC/ μ l] in practical worldwide use.

The purpose of this paper is to describe the improvements on the ICC method to give a higher accuracy and extend the upper limit of measurement to the sufficient level for practical use. We evaluate the centrifuge concentration process, one of the important processes of the ICC method, by computer simulation in order to investigate the factor determining the upper limit of measurement of the ICC method. The standard leukocyte fluorescence image profile is subsequently established so that an optimum image analysis algorithm is developed. Furthermore, we verify the effect of our improvement by comparing the leukocyte counts by the ICC method with those of the Nageotte hemocytometry. As a result of the experiments, miss-counting of the dusts was markedly decreased, and the linearity of leukocyte counts increased up to 25 [WBC/ μ l].

2. Description of the ICC method

We briefly explain the ICC method and describe additional improvements below. Schematic diagram of the ICC method is shown in Fig. 1. Generally, erythrocytes or platelets, and contaminating leukocytes exist in a blood product. A surface-active reagent, Triton X-100, is used to dissolve platelets, erythrocytes, and the cell membranes of leukocytes simultaneously.

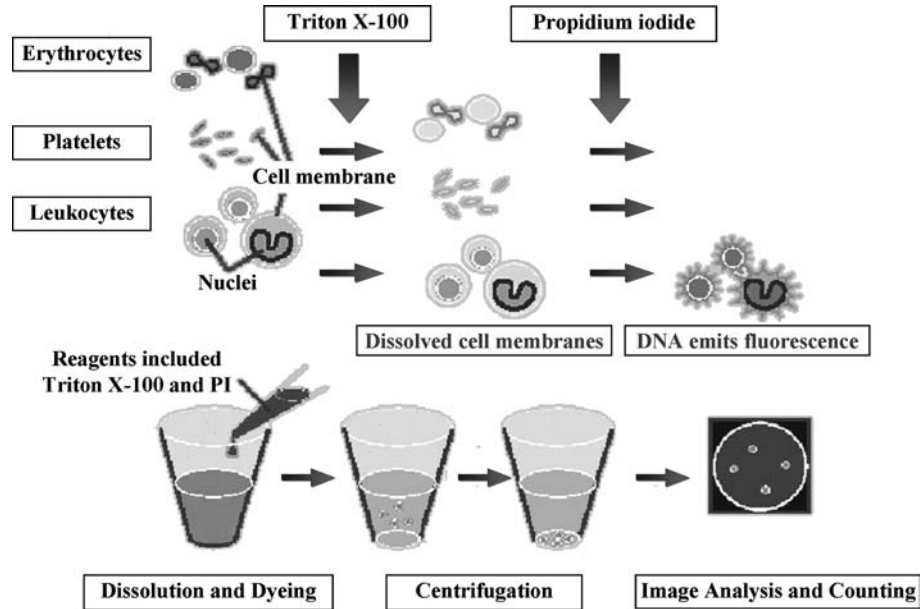


Fig. 1. Principle of measurement of the ICC method. Erythrocytes or platelets, and contaminating leukocytes exist in a blood product. A surface-active reagent, Triton X-100, is used to dissolve platelets, erythrocytes, and the cell membrane of leukocytes. PI can be intercalated into nucleic DNA of leukocytes so that only leukocytes can be stained to emit fluorescence. In practice, blood and the reagent, including Triton X-100 and PI, are mixed in a cuvette, then it is centrifuged to drop all leukocytes onto the bottom surface of the cuvette. Thus, leukocyte fluorescence image can be obtained.

Propidium iodide (PI) can be intercalated into nucleic DNA of leukocytes so that only leukocytes can be stained to emit fluorescence. In practice, blood and the reagent including Triton X-100 and PI, are mixed in a cuvette. Then, it is centrifuged to drop all leukocytes onto the bottom surface of the cuvette with the diameter of 2 mm. In our system, swing bucket type, not fixed angle type, rotor is used to drop leukocytes uniformly to the whole area of the bottom (for example, combination of A12-11 rotor and 5417 centrifuge, both Eppendorf, Co. Ltd, is recommended). Thus, leukocyte fluorescence image can be obtained by imaging the bottom of the cuvette. The key step in this method is centrifugal concentration of leukocytes onto the bottom surface of the cuvette. All leukocytes are concentrated in the small 2 mm ϕ circular imaging area by centrifugation.

System configuration of the ICC method is shown in Fig. 2. A SHG of Nd:YAG laser (HK-9755, Shimadzu Corp., Japan) emitting light with the wavelength of 532 nm is used as an excitation light source. In the case of PC samples, the excitation laser beam irradiates the sample from side direction to reduce background noise signal. On the other hand, in the case of RC samples, it irradiates from the bottom direction with rotating mirror placed

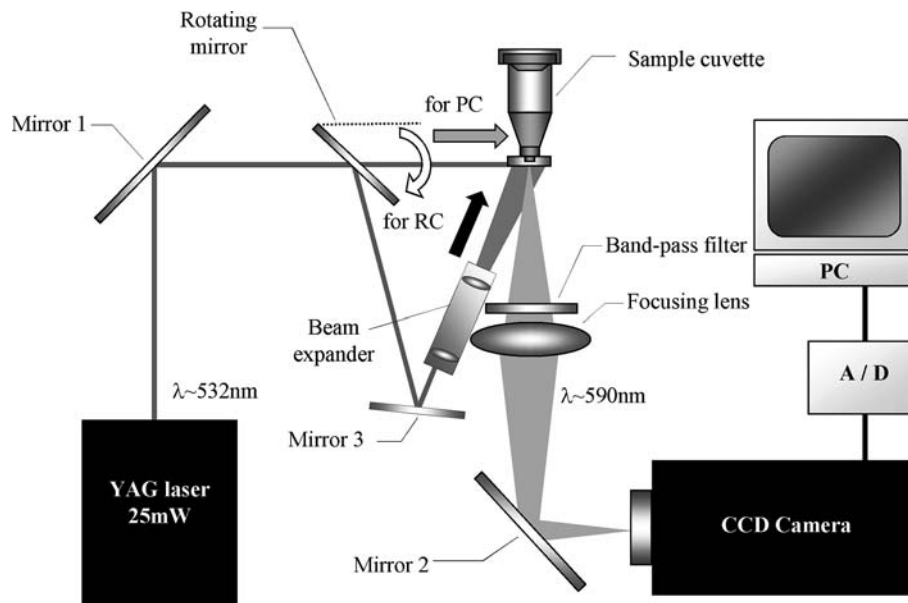


Fig. 2. System configuration of the ICC method. A green YAG laser ($\lambda = 532 \text{ nm}$) was used as an excitation light source. Two types of irradiation modes were switched by a rotating mirror: side irradiation mode was used for PC samples, and bottom irradiation mode for RC samples. Fluorescence wavelength was approximately 590 nm. Fluorescence image was detected by a CCD camera via an optical band-pass filter. The image was converted to digital data and led to personal computer. It was analyzed by a software on the personal computer to recognize and to count leukocytes.

at the incidental optical path before the sample cuvette. Since fluorescence with the wavelength around 590 nm is emitted from leukocyte nuclei, fluorescence images can be obtained by a $1/2'$ type monochromatic CCD camera (BE-IR20N-S4, Hitachi Kokusai Electric Inc., Japan), with the effective pixel number of 768×494 pixels (imaging area: $6.45 \times 4.84 \text{ mm}$), via an optical band-pass filter. This optical filter selectively transmits the light with the wavelength of $590 \pm 40 \text{ nm}$ (FWHM), so that it can extract the fluorescence light by separating from the excitation light. Since the magnification of the whole lens system is 2.2-fold, $4.6 \mu\text{m}$ -length is approximately imaged onto the 1 pixel of the CCD camera sensor. Then, the image is digitized to 640×480 pixel image and captured into a computer. Figure 3 shows fluorescence image of leukocytes obtained by the ICC method. It is analyzed using an image analysis technique to recognize leukocytes to be counted.

3. Fluorescence image profiles for leukocyte and dust

At first, we started to create a standard fluorescence image profile of the leukocyte obtained by the ICC method. In this section, we describe the

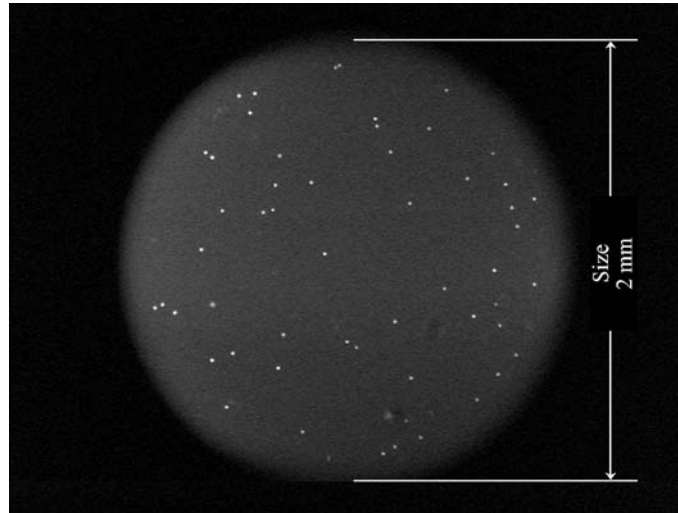


Fig. 3. Fluorescence image by the ICC method. Images with 1 pixel resolution of $4.6\ \mu\text{m}$ and intensity level of 256 are obtained by the ICC method. The gray circular area is the background due to the spontaneous fluorescence of PI. Leukocytes are displayed as white points in the circle.

method to create it, and also explain a result of investigation for cause of its shape.

3.1. STANDARD LEUKOCYTE FLUORESCENCE IMAGE PROFILE

After processing by the reagent under the optimum chemical conditions, several fluorescence images of the leukocytes were obtained, and more than 100 image profiles of leukocyte image signals were extracted and collected manually. Each profile covered total 16 by 16 pixels including the surrounding background signals. Both of PC and RC samples were investigated to create the standard profiles. Taking the average of all data, we created the 'standard leukocyte profile'. In order to discriminate the leukocytes from the dusts, the dust profiles were also collected and created.

Finally, we created a standard fluorescence image profile of leukocyte using the measured profile. This standard profile is thought to be formed due to fact that eukaryotic DNA is normally localized as a chromatin with winding around histone protein molecules and packaged in nucleus, so that the nucleus can be assumed to have a spherical shape, and fluorescent dye would be uniformly distributed in the nucleus.

Then the fluorescence intensity observed in a 2D plane can be calculated by integrating the fluorescence intensity along the line perpendicular to the observing 2D plane as shown in Fig. 4(a). Here we assumed the fluorescent light is not self-absorbed by the nucleus.

There are two factors which influence the intensity profile of the leukocyte such as: (1) internal absorption and (2) influence of fluorescence emitted from pile of leukocytes. In the case of (1), a leukocyte emits fluorescence and it goes through inside of the leukocyte with absorption. However, fluorescence, of which wavelength is about 590 nm, would not be absorbed by leukocyte, it was estimated that at least 99.99% of light can be penetrate through 20 μm diameter of a leukocyte. Thus, the influence in this case can be neglected. Considering the case of (2), we calculated the average distance

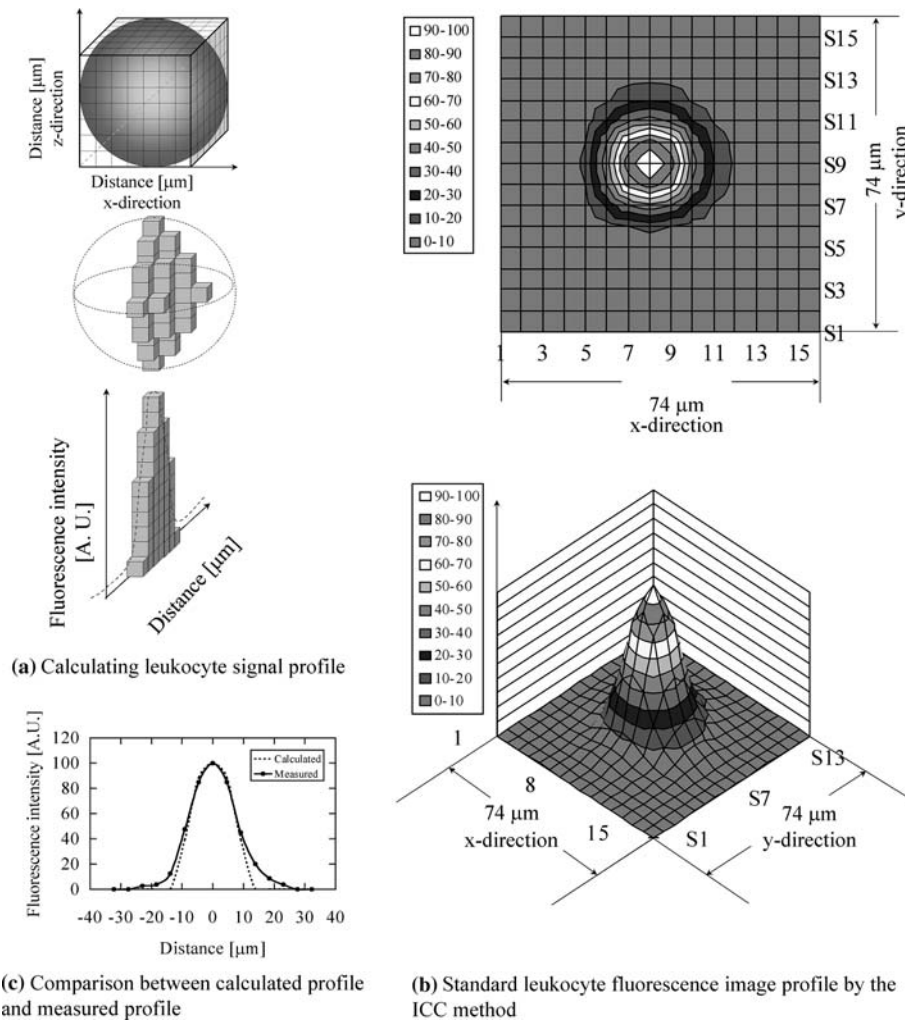


Fig. 4. Consideration of leukocyte fluorescence image profile. (a) Since eucaryotic DNA is normally localized as spherical shape, fluorescence intensity can be calculated to integrate the sphere with projecting onto 2D. (b) The closed circles and the solid line represent the measured data, and the dashed line represent calculated. (c) Leukocyte cell model was found to be sphere with a diameter of approximately 20 μm .

between the neighboring leukocyte. In establishment of the standard leukocyte fluorescence image profile, actual leukocyte fluorescence images were collected from fluorescence images like as Fig. 3. The number of leukocytes included in each image was less than 100 leukocytes. As described below in Section 4.2, leukocytes placed in the upper conical zone before centrifugation were concentrated in the peripheral annular region of the bottom plane after centrifugation. The volume of the conical zone is 23.89 mm^3 , and this is about 51% of that of the whole volume of the cuvette, that is, $23.89 + 7.27\pi = 46.72 \text{ mm}^3$. Therefore, if 100 leukocytes are suspended in the whole solution, about 51 leukocytes exist in this zone. These leukocytes drop to the peripheral annular region of the bottom plane by centrifugation. Since 51 leukocytes with the shape of $20 \mu\text{m}\phi$ sphere are assumed to exist in the region, It means that 51 leukocytes exist in the circumference of the bottom of the cuvette (radius $r = 1 \text{ mm}$), so that, $2\pi r = 6 \times 10^{-3}$. And $6 \times 10^{-3}/51 = 100 \mu\text{m}/\text{cell}$. Since average distance between adjacent $20 \mu\text{m}\phi$ leukocytes is $100 \mu\text{m}$, the probability of overlapping of them is considered to be very low. Similarly, in the central region, the remaining 49 leukocytes exist in the area of $\pi(1 - 0.020)^2 = 3.02$, $3.02 \times 10^6/49 = 6 \times 10^4 \mu\text{m}^2/\text{WBC} = (240 \mu\text{m})^2/\text{cell}$. Since it means there is only one $20 \mu\text{m}\phi$ leukocyte in a square with sides $240 \mu\text{m}$ on average, the probability of overlapping of them can also be considered to be very low. Therefore, the self-absorption of fluorescence and pile of cells can be assumed negligible.

On the other hand, the measured standard profile of leukocyte is shown in Fig. 4(b). We compared the simulated standard profile with the measured one and obtained a good agreement as shown in Fig. 4(c) if the diameter of the leukocyte DNA is assumed to be $20 \mu\text{m}$. Thus, although the size of leukocyte seems to be $30 \mu\text{m}$ from the results of the measured standard profile of leukocyte, it would rather be considered as $20 \mu\text{m}$ diameter sphere.

3.2. FLUORESCENCE IMAGE PROFILE OF DUSTS

Typical 'dust' profile is shown in Fig. 5. Although dusts could be classified into three categories, (1) distorted shapes, (2) String-like shape, and (3) Chaff-like shape, they have a common characteristic of high backgrounds. In general, since the dust tends to exist over a wide area, the true background cannot be identified. These facts were utilized to develop the double thresholding algorithm described in the next section.

4. Improvements on leukocyte counting

We have two problems to improve the accuracy and linearity of leukocyte counting of the ICC method. One is excess-counting of dusts as leukocytes

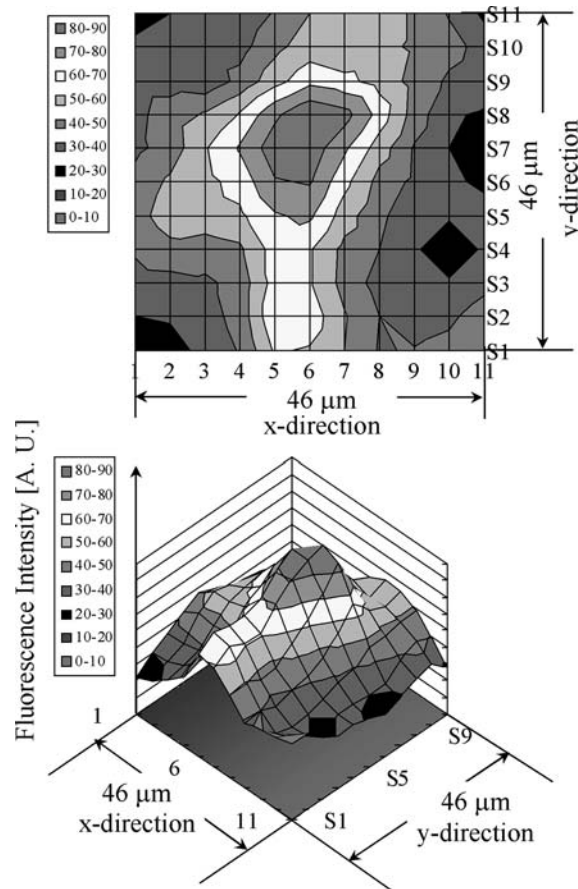


Fig. 5. Typical fluorescence image profile of a 'dust'.

in error. The other is miss-counting of overlapped leukocytes after centrifugation of blood samples contained in a cone-shape type of cuvette. These problems are solved by double thresholding of fluorescence image profile and by a correcting method of the leukocyte overlapping established on the basis of centrifugation process simulation.

4.1. DOUBLE THRESHOLDING

We developed a 'double thresholding' algorithm and implemented it in the software for correct leukocyte recognition to avoid counting dusts in error. Fig. 6(a) explains the principle of this algorithm. The solid curve shows the standard 'leukocyte profile', and the dotted curve indicates a typical 'dust profile', with a distorted shape. In the previous ICC method, only upper

threshold was used to discriminate candidate objects for leukocytes from the background because no dusts were found. It is supposed that the peak intensities of leukocytes, I_m , obey the Gaussian distribution. The Gaussian distribution can be approximated to a Poisson distribution for large number of event, that is, the peak intensity in our case, so that the standard deviation (SD) can be calculated by taking the square root of the mean value (Watson 2001). Investigating the total 145 profiles of the leukocyte image profiles which were used in creating the standard image profile, the mean value of the peak intensities was calculated to $I_m = 100.20$ in an arbitrary unit, and the $SD = 8.97$. Since the square root of I_m is close to the SD, approximating the Gaussian distribution to the Poisson is acceptable, and the SD is estimated to be $\sqrt{I_m}$. Then, the probability that a peak intensity of leukocyte has its intensity in the range of $I_m \pm SD$ is 68%. Approximately 95% of the peak intensities lie within $I_m \pm 2SD$ and 99.99% lie within $I_m \pm 4SD$. Then, in order to pick up candidate objects with more than 99.99% confidence, the upper threshold was given as $I_m - 4SD = I_m - 4\sqrt{I_m}$.

However, using the upper threshold only, indicated by the single-dotted line, is difficult to distinguish dust from the leukocyte because the width at the upper threshold w_{d1} for dust is close to that for leukocyte w_{l1} in Fig. 6. Histogram of pixel intensity of the whole image is created and the background intensity is estimated by taking the intensity at the peak of the histogram as shown in Fig. 7. Then, the lower threshold is determined by 1.5 multiplying the background intensity to leave margins and applying it. At the lower threshold (the double-dotted line) the widths w_{d2} of dust are very different from that of leukocyte, w_{l2} , and dusts can be easily distinguished from leukocytes.

Figure 6(b) (i) and (ii) shows the intensity profiles in the 2D plane for typical leukocyte (i) and dust (ii). The pixels with the intensity higher than the upper threshold ($= 145$) is presented as dark gray, and those between the upper and the lower thresholds ($= 128$) presented as light gray. In Fig. 6(b) (i), for leukocyte, the dark and light gray pixels are close to each other. On the other hand, for the case of dust in Fig. 6(b) (ii), the light gray area is much wider although the dark gray area is almost the same as that of the leukocyte.

Figure 8 compares the area ratios S_L/S_U for leukocytes (closed circle) and dusts (open circle), where S_U is the number of pixels with the intensity over the upper threshold (area of dark gray in Fig. 6(b)), and S_L that between the upper and lower thresholds (area of light gray in Fig. 6(b)). In Fig. 8, the area ratios S_L/S_U are plotted as a function of S_L . It is seen that the ratios for the leukocyte are much smaller than those for the dusts, and we can clearly find a reference value to demarcate dusts from leukocyte as shown by the dashed line. In practice, the area ratio (S_L/S_U) for each candidate object is calculated and evaluated to recognize the leukocyte, that is,

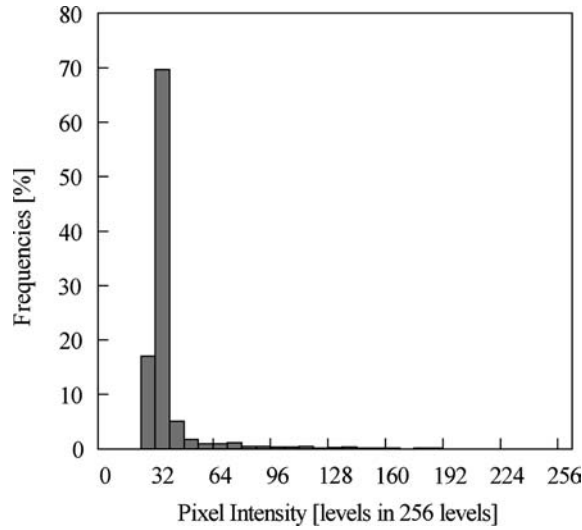


Fig. 7. Histogram of pixel intensities. Typical histogram of intensities of each pixel of a fluorescence image obtained by the ICC method is shown. The peak around the intensity level of 32 indicates the background, The lower threshold is calculated by this value of background plus some margin.

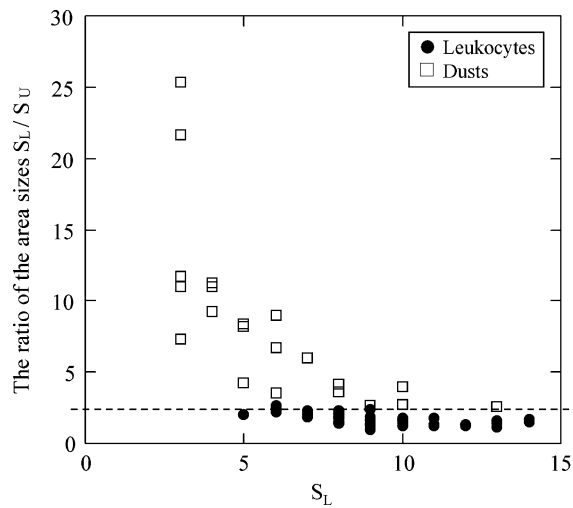


Fig. 8. Demarcation between leukocytes and dusts by the area ratio S_L/S_U . The ratio of the area with the lower threshold S_L , to the area with the upper threshold, S_H , were plotted against S_L . The closed circles represent the data of leukocytes, and the open squares represent dusts S_L/S_H of leukocytes are found to be lower than that of dusts so that the discrimination level can be determination as shown with the dashed line.

cone. Then, after centrifugation, the distributions of leukocytes and dusts at the column bottom are not homogeneous, but denser at the outer area than the central area. In the denser area some leukocytes may be overlapped or piled up and the multiple leukocytes may be miss-counted as one leukocyte. However, it is not observable how each leukocyte drops to the bottom of the cuvette. Therefore, we tried to simulate the centrifugation process to make a relation to correct the miss-counting of overlapped leukocytes.

Simulation was performed in the following procedure.

At first, a cuvette model was generated based on the size of an actual cuvette. It has 20° tilting on one side at the upper part, forming the conic zone and circular column at the lower part as illustrated in Fig. 9(a). In adding $40 \mu\text{l}$, (assuming $20 \mu\text{l}$ of reagent and $20 \mu\text{l}$ of sample) solution, the total height of the solution becomes about 7.27 mm , that is 4.0 mm height for circular column and about 3.27 mm for conic zone.

Next, this model cuvette was divided into the small volume elements as shown in Fig. 9(b) and (c). The volume of each element was set to the same as that of the leukocyte nuclei, approximately $-8000 \mu\text{m}^3$ ($-20 \mu\text{m}\phi$, which is found in the standard leukocyte image profile described in Section 3. To keep the volume of each element the same, (1) 7.27 mm height was sliced to disks with a height of $20 \mu\text{m}$. (2) Each disk was radially divided into concentric annuli with a width of $20 \mu\text{m}$. (3) Each disk was again

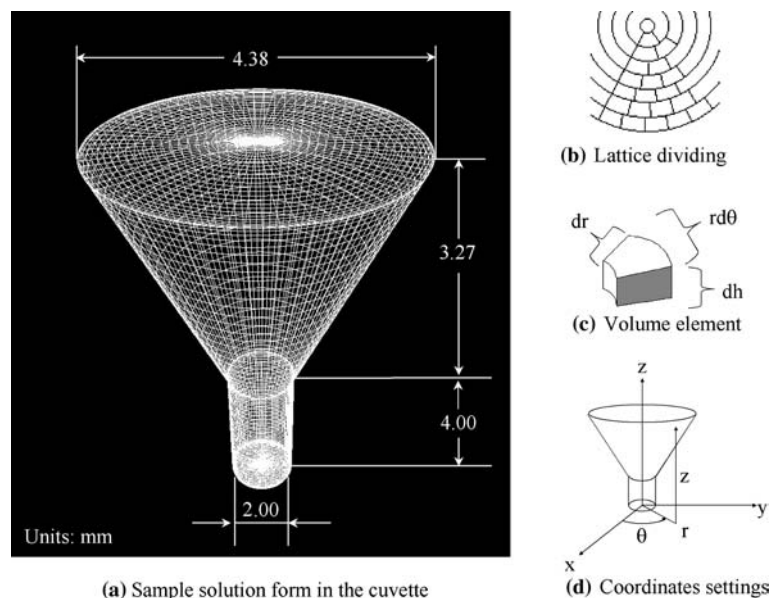


Fig. 9. Settings of simulation.

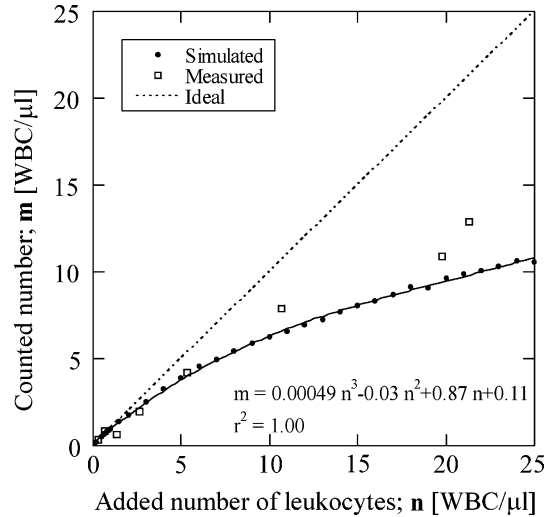


Fig. 10. Simulation result and the measurement limit in leukocyte counting by the ICC method. The open squares represent the measured data. The closed circles represent the calculated data as results of our simulation. They were fitted with three orders polynomials as solid line. The dashed line represents the ideal values that indicates the true numbers of added leukocytes. The number density of leukocytes were found to be less than true values in the range of over 10 [cells/ μ l] by the ICC method. Simulation results were consistent with the measured data.

divided along the angular direction with the arc of each element, ($r d\theta$ of 20 μ m). (4) all elements were numbered for identification.

We chose the cylindrical coordinates (r, θ, z) as shown in Fig. 9(d). Using this coordinate system, the virtual leukocytes are arranged within the partitioned cuvette as follows. (1) The number of the leukocytes is given at first. (2) Next, the required sets of random numbers are generated. (3) A virtual leukocyte was placed in the element at the coordinate where the random number indicates. It is ruled that one element is occupied by only one leukocyte. (4) These procedures are repeated until all leukocytes are arranged.

Then, the centrifugation is simulated numerically. The dropping pathways of leukocytes by the centrifugation are assumed as follows: (1) z coordinate of each leukocyte is changed to 0, which means the leukocyte is dropped onto the bottom. (2) If a leukocyte collide with the wall of the conic zone in the way, r coordinate is moved to 2mm, which means the leukocyte existing at the peripheral conic zone at the beginning is concentrated to the peripheral area of the bottom of the circular column after the centrifugation. (3) If not, the leukocyte is dropped keeping its r coordinate.

After centrifugation simulation, the number of the leukocytes are counted at the bottom of the cuvette. If multiple leukocytes are overlapped at the same position of the bottom of the cuvette, they are also counted as one for the case of fluorescence images.

Figure 10 shows the results of the simulation. It is found that if the number density of leukocytes per micro liter exceeds 5 [WBC/ μ l], the number of leukocytes detected by the ICC method becomes less than the true value. Leukocyte cells floating at the peripheral area of upper tilting zone of the cuvette may collide each other at the bottom of the cuvette after centrifugation. This collision causes miss-counting of the cells and limits the measurement range of the leukocytes density by the ICC method. From the results of Fig. 10, we found that the counted number m can be expressed by a third order polynomial of n , the added number of the leukocytes in a cuvette, as

$$m = 0.00049n^3 - 0.030n^2 + 0.87n + 0.11, \quad (r^2 = 1.00), \quad (1)$$

where m is less than n in the range of n larger than 5 [WBC/ μ l], but fortunately, it increases monotonically in the range we tested. Thus, we can obtain n numerically by inverting the above equation as Equation (2).

$$n = 0.0045m^3 + 0.082m^2 + 0.91m + 0.034. \quad (r^2 = 1.00). \quad (2)$$

We use Equation (2) to develop a correction method to extend the measurement range. Finally, the algorithm for the ICC method incorporates the double thresholding and the correction for overlapping.

5. Experimental verification

The effect of the developed leukocyte recognition algorithm was evaluated by experiments with actual blood samples. The leukocyte counts measured by the ICC method were compared with those by the conventional Nageotte hemocytometry.

5.1. MATERIALS AND METHODS

5.1.1. Sample preparation

5.1.1.1. *Collection of blood.* Blood was collected from healthy voluntary donors using ACD-A for PC samples or CPD for RC samples as anticoagulants. Whole blood was centrifuged at $150 \times G$ for 15 min at the room temperature.

5.1.1.2. *Preparation of PC samples.* After centrifugation, the supernatant, platelet-rich plasma (PRP) was collected without disturbing the other fractions. Required volume of the PRP was taken, and the remainder was

centrifuged at $1500 \times G$ for 5 min at the room temperature to prepare platelet-poor plasma (PPP). PPP was filtered ($0.2 \mu\text{m}\phi$ pore filter, New Steradisc, Kurabo, Japan) to remove leukocyte completely, and was used as diluents for Platelet samples. We prepared a dilution series of platelet samples with the PRP and the PPP solution.

5.1.1.3. *Preparation of RC samples.* Buffy coat was removed from the RBC solution after the first centrifugation. And, MAP solution was added to the RBC solution so that RC-MAP solution, which was used mainly in Japan, was prepared (AABB 2002). Being similar to PC samples, some RC-MAP was taken, and the remainder was filtered twice to remove leukocytes using the leukocyte-reduction filter for RC products (RC-NE01J, Nihon Pall Ltd., Japan). The double-filtered RC-MAP was used as diluents for RBC samples. We also prepared a dilution series of RC-MAP samples with the RC-MAP and the double-filtered RC-MAP.

5.1.2. *Nageotte hemocytometry*

5.1.2.1. *PC samples.* Fifty microliter of the blood sample and $200 \mu\text{l}$ of Türk solution (Wako Pure Chemicals Industries, Ltd., Japan) are mixed well in the Eppendorf centrifugal tube to stain leukocytes. After leaving for 5 min, the mixed solution was inserted into the Nageotte chamber. Since the counting volume of the Nageotte chamber was $50 \mu\text{l}$, the net volume of the samples became $10 \mu\text{l}$. To drop all leukocytes, the samples left for 15 min in a humid environment (relative humidity was more than 82% at room temperature). And then, leukocytes were counted manually under the microscopy. It took about 20–30 min per sample to count the leukocyte on average (AABB 1996).

5.1.2.2. *RC samples.* Four hundred and fifty microliter of Leukoplate solution (SOBIODA, France) for $50 \mu\text{l}$ of the blood sample are used to stain leukocytes. After leaving for 10 min, the mixed solution was inserted into the Nageotte chamber. The net volume of the samples became $5 \mu\text{l}$ in RC samples. After further leaving for 30 min in a humid environment (relative humidity was more than 82% at room temperature), leukocytes were counted similar to the PC samples (AABB, 1996).

5.1.3. *Leukocyte counting by the ICC method*

Twenty microliter of the reagent containing surface-active reagent and fluorescent dye was mixed with the same volume of the blood sample well in a cuvette to dissolve the cell components and to stain the nuclei of the leukocytes. Then the cuvettes were centrifuged at $2700 \times G$ for 2 min at room temperature. Two types of programs were compared. One (new) incorporate the double thresholding and the correction of overlapping. The

other (old) uses only the upper thresholding. To compare these software each other, same sample cuvette were measured by both versions. To cancel the deterioration of the samples, the fluorescence images were stored in the hard disk drive, and then the stored images were counted using the both software.

5.2. RESULTS AND DISCUSSION

Figure 11 shows number of leukocytes measured by the ICC method with (closed circles) and without (open squares) the double thresholding algorithm, plotted for true number calculated from the results by Nageotte hemocytometry. Figure 11(a) shows the results for the PC samples and (b) for the RC samples. The double thresholding algorithm was highly effective for precise leukocyte counting for RC sample (b). In contrast, a little improvement was found for PC sample (a). This was due to a few dusts contained in the prepared PC samples in fact because of the $0.2\ \mu\text{m}\phi$ filtration, as opposed to RC samples. However, since the practical PC transfusion blood product might contain the dusts, this algorithm would be likely to useful in testing the practical PC blood products.

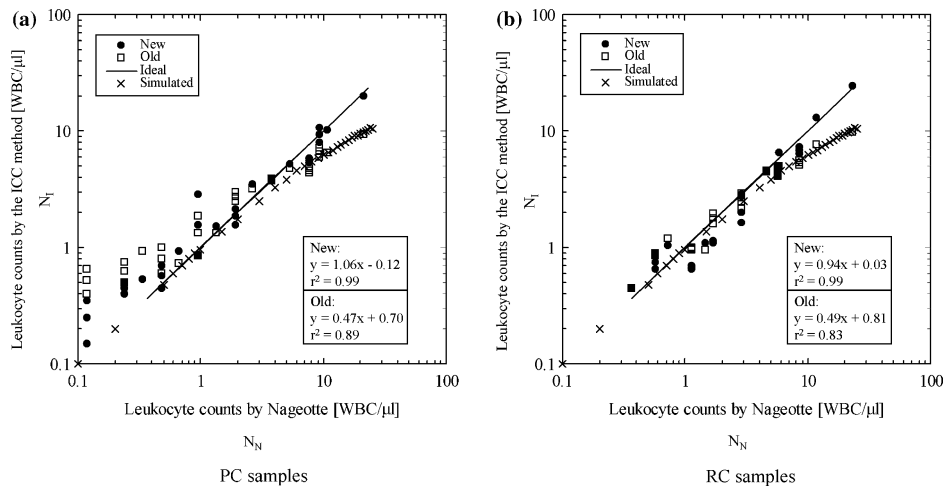


Fig. 11. Comparison of the leukocytes counts by the ICC method with and without double thresholding algorithm. Number of leukocytes measured by the ICC method with (closed circles, new) and without (open squares, old) the double thresholding algorithm and the correction of the leukocyte overlapping are plotted for true number calculated from the results by the conventional Nageotte hemocytometry. The data with new algorithm were fitted with the least square method. They are found to be in good agreement with the ideal values calculated from the results by the Nageotte hemocytometry represented by the solid line. It was found that the measurement range was extended up to 25 [WBC/ μl].

In addition, the linearity of the data with the new algorithm are found to be kept in the range up to 25 [WBC/ μ] for both samples. It is due to the correction method obtained from the results of the simulation. The data with the new software implementing both the double thresholding algorithm and correction method in the range over 5 [WBC/ μ], were fitted with the least square method. Regression lines were calculated as $y = 1.06x - 0.12$ ($r^2 = 0.99$) for the PC samples, and $y = 0.94x + 0.03$ ($r^2 = 0.99$) for the RC samples. The data processed by the old software, represented as open squares, lie below the ideal line in the range over 5 [WBC/ μ] for both the PC and RC samples (each regression line was calculated as $y = 0.47x + 0.70$ ($r^2 = 0.89$) for the PC samples, and $y = 0.49x + 0.81$ ($r^2 = 0.83$) for the RC samples). These data from the old algorithm agree well with those of results of the simulation, represented as the crosses in Fig. 11(a) and (b).

Table 1. Contribution of the overlapping correction and the double thresholding

Overlapping Correction	Double thresholding	
	-	+
(a) PC samples		
-		
whole range	$y = 0.47x + 0.70$ $r^2 = 0.89$ (-, -)	$y = 0.48x + 0.60$ $r^2 = 0.88$ (-, +)
below 1[WBC/ μ]	$y = 1.07x + 0.02$ $r^2 = 0.71$ (-, -)	$1.10x + 0.00$ 0.88 (-, +)
+	$y = 1.07x - 0.09$ $r^2 = 0.99$ (+, -)	$y = 1.06x - 0.12$ $r^2 = 0.99$ (+, +)
(b) RC samples		
-		
whole range	$y = 0.49x + 0.82$ $r^2 = 0.83$ (-, -)	$y = 0.47x + 0.69$ $r^2 = 0.89$ (-, +)
below 1[WBC/ μ]	$y = 1.05x + 0.12$ $r^2 = 0.86$ (-, -)	$y = 1.04x + 0.03$ $r^2 = 0.94$ (-, +)
+	$y = 0.93x + 0.20$ $r^2 = 0.99$ (+, -)	$y = 0.94x + 0.03$ $r^2 = 0.99$ (+, +)

To investigate the contributions of the two improving methods, i.e. the overlapping correction and the double thresholding, the equations of the regression lines and the correlation coefficients of four combination cases are summarized;

(i) neither the overlapping correction nor the double thresholding (-, -) (ii) only the overlapping correction (+, -), (iii) only the double thresholding (-, +), (iv) both methods are applied (+, +), for (a) PC and (b) RC samples.

For both samples, the overlapping correction is found to be effective for increasing the slopes of regression lines. It means the overlapping correction is effective for extending the measuring range up to 25 [WBC/ μ].

On the other hand, the double thresholding is effective for achieving higher accuracy with removing the miss-counting of dusts as shown that the correlation coefficients approach to 1 in the range below 1[WBC/ μ].

The correlation coefficients of the data with the new software are higher than those with the old software for both types of samples.

Table 1 summarized the equation of the regression lines and correlation coefficients in various combinations of the two new methods, the double thresholding and the overlapping correction, to make the contribution to the improvement of each method clearer. We examined four cases, i.e., (i) neither the overlapping correction nor the double thresholding (–, –) is employed (the old algorithm), (ii) only the overlapping correction (+, –), (iii) only the double thresholding (–, +), and (iv) both methods (+, +) as shown in Fig. 11 above. For both (a) PC and (b) RC samples, the overlapping correction was found effective to make the slopes of the regression lines close to 1. On the other hand, the double thresholding seemed to be ineffective for more accurate leukocyte counting. This was considered to be due to calculating regression equation using all data including out of linearity range. Then, it was calculated again using the data in the range below 1 [WBC/ μ l] only. As the results, it is found in both samples that the correlation coefficients become higher by employing the double thresholding. Thus, the double thresholding was effective for increasing accuracy in leukocyte counting. Therefore, both the two methods are required for improving the accuracy and the measuring range of the ICC method.

6. Conclusions

We developed a leukocyte counting method based on centrifugal concentration of leukocytes into a small area and the fluorescence image analysis technique. This centrifugation process was simulated to understand the phenomenon and to develop a correction method for overlapping of leukocytes. A standard leukocyte fluorescence image profile was created to discriminate leukocytes from dusts using the double thresholding method. These two methods were incorporated with a new algorithm for leukocyte counting. The double thresholding method was found to be effective for preventing from miss-counting of dusts, particularly in the RC samples. The overlapping correction was found to extend the linearity of the ICC method against the leukocyte concentration up to 25 [WBC/ μ l]. Thus, the ICC method, including these techniques, would be powerful tool to count leukocytes for quality control of the transfusion blood products.

Acknowledgement

We would like to thank Dr M. Ishikawa, Y. Ichihashi, T. Takayanagi, K. Mitsumoto, Y. Kato, Y. Sugiura, M. Yoshimura, H. Okada, and

Dr T. Nagoya, who were members of the biomedical group of life science division of Kowa Company, Ltd, for valuable discussion, for cooperation, and for their encouragements.

References

- AABB, *Blood Transfusion Therapy: A Physician's Handbook*, 7th edn., p. 80, 2002.
- AABB Technical Manual, 12th edn., Bethesda, AABB, p. 722, 1996.
- Adams M.R., D.K. Johnson and M.P. Busch. *Transfusion* **37** 29, 1997.
- Blood Products Advisory Committee, Summary for Topics II, Gaithersburg, MD, December 13–14, 2001, <http://www.fda.gov/ohrms/dockets/ac/01/briefing/3817b1.06.williams1.pdf>
- Dizik S. *Transfus. Med. Rev.* **11** 44, 1997.
- Nagahashi, H.K. Yabusaki, H. Matsui, T. Hirono, N. Yokokawa, M. Satake, K. Tadokoro and T. Juji. *Vox Sang* **79** 34, 2000.
- Neumuller, J., D.W.M. Schwartz and W.R. Mayr. *Vox Sang* **73** 220, 1997.
- Yabusaki, K., T. Hirono and H. Matsui. XIIth International Symposium on Technological Innovations in Laboratory Hematology, Workshop on New Technology in Laboratory Hematology, Kobe, Japan, September 9–11, **79**, 1999.
- Yabusaki, K., N. Saitoh, T. Hirono, H. Matshui and H. Okada, *Jpn. J. Appl. Phys.* **39** 3641, 2000.
- Watson, J.V. *Cytometry (Communications in Clinical Cytometry)* **46** 1, 2001.